C1.2 Flow over the NACA0012 airfoil, inviscid and viscous, subsonic and transonic

Aravind Balan*, Georg May, and Michael Woopen
RWTH Aachen University, Germany

1 Code Description

We use a hybridized discontinuous Galerkin method as described in [2]. The globally coupled unknowns are the so-called hybrid variables, i.e., functions having its support on the skeleton of the mesh. The 'classical' variables appearing in standard discontinuous Galerkin methods, such as the unknown function on the mesh, can, similarly to lifting operators, be written as functions of the hybrid variables. Depending on the polynomial degree, any (formal) order of consistency with the Navier-Stokes equations (or Euler equations, respectively), can be achieved. So far, we are not able to run the code in parallel.

To solve the resulting nonlinear system of equations, we use a (damped) Newton's procedure. The occurring linear system of equations is solved with a restarted GMRES solver (30 search directions) with ILU preconditioning. The ILU depth is chosen to be 3. The systems are solved with a relative tolerance of 10^{-4}. We use PETSc for the solution process.

Expressing the unknown function on the mesh via hybrid variables necessitates the solution of multiple (comparably) small linear systems of equations. We solve these systems exactly with LAPACK routine dgesv.

Our method is based on a Galerkin formulation and adjoint consistent, so we can use a dual-weighted residual approach for adaptation. If the primal solution is computed with order p, the dual solution is computed with order $p+1$ on the same grid. In addition to an adaptation criterion, the dual approach also yields an estimate for the error in some specified target functional under consideration. This can be used to enhance the quality of the latter. Anisotropic mesh adaptation is performed where the anisotropy is found from the $(p+1)$-st derivative of the solution.

2 Case Summary

Three cases of flow over NACA 0012 airfoil are considered

- Subsonic inviscid flow, $M_\infty = 0.5, \alpha = 2^\circ$
- Transonic inviscid flow, $M_\infty = 0.8, \alpha = 1.25^\circ$
- Subsonic viscous flow, $M_\infty = 0.5, \alpha = 1.0^\circ, Re = 5000$

The geometry of the airfoil is defined by

$$y = \pm 0.6(0.2969\sqrt{x} - 0.1260x - 0.3516x^2 + 0.2843x^3 - 0.1036x^4) \tag{1}$$

*balan@aices.rwth-aachen.de

with $x \in [0, 1]$. The mesh was created using the Netgen mesh generator[1]. The far field is a circle, centered at the airfoil mid chord with a radius of 1000 chords. The initial mesh for both the inviscid and viscous flow simulations have 2155 triangular mesh elements (Fig 1).

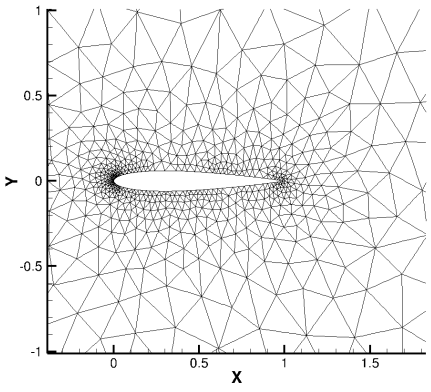

Figure 1: Initial mesh - 2155 elements

3 Results

For the subsonic inviscid case, the reference values were obtained using adaptive isotropic hp-refinements, with number of solution degrees of freedom of around 2.6×10^5 and 1.9×10^5 for drag coefficient, $c_{d_{ref}}$ and lift coefficient, $c_{l_{ref}}$, respectively. Those reference values are given as

$$c_{d_{ref}} = 4.664270 \times 10^{-6} \quad (2)$$

$$c_{l_{ref}} = 2.864086 \times 10^{-1} \quad (3)$$

Fig. 2 shows the drag-adapted mesh after 6 adaptations for $p = 3$. Fig. 3 shows the convergence of the error in the drag coefficient as we vary the polynomial degree. For higher p, the convergence rate has become better. In terms of the work units too, higher p seems to pay off. Fig. 4 shows the convergence of the error in the lift coefficient for different polynomial degrees. Like in the drag coefficient case, here also the convergence rates for $p = 2$ and $p = 3$ are better than that of $p = 1$. However the convergence is not as smooth as the one for the drag. This could be probably because of the high influence of the singularity at the trailing edge of the airfoil.

For the transonic inviscid case, the reference values were obtained using adaptive isotropic hp-refinements, with number of solution degrees of freedom of around 2.3×10^5 and 2.8×10^5 for drag coefficient, $c_{d_{ref}}$ and lift coefficient, $c_{l_{ref}}$, respectively.They are given as

$$c_{d_{ref}} = 2.274636 \times 10^{-2} \quad (4)$$

$$c_{l_{ref}} = 3.529140 \times 10^{-1} \quad (5)$$

Fig. 5 shows the drag-adapted mesh after 9 adaptations for $p = 2$. As one would expect, the regions, which contribute most to the error, such as the upper shock, the lower shock, the trailing edge singularity, and the high-gradient leading edge got refined.

Fig. 6 shows the convergence of the error in the drag coefficient as we vary the polynomial degree. As we increase the polynomial degree beyond 2, there is hardly any difference. This

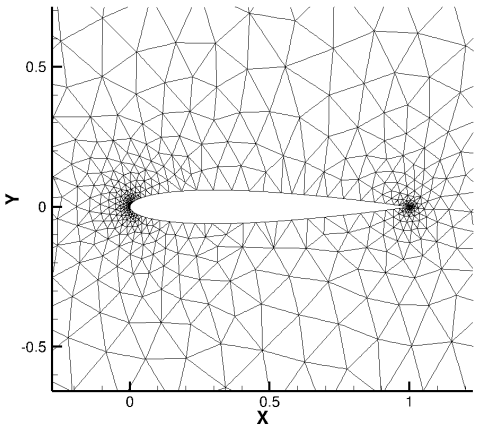

Figure 2: Adapted mesh (1775 elements) for drag coefficient as target function for the inviscid subsonic flow

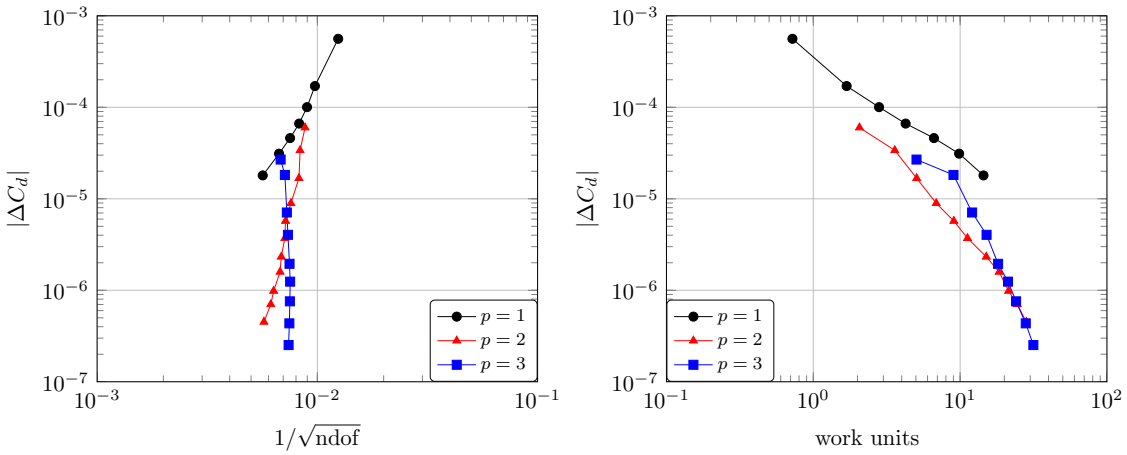

(a) Error in drag coefficient Vs Degree of freedom

(b) Error in drag coefficient Vs Work units

Figure 3: Inviscid subsonic flow, $M_\infty = 0.5$, $\alpha = 2^\circ$

should be because of the discontinuities in the transonic flow. In terms of the work units too, higher p does not give faster results. Fig. 7 shows the convergence of the error in the lift coefficient for different polynomial degrees. Like in the case of drag coefficient, increasing the polynomial degree beyond 2 does not increase the rate of convergence.

For the subsonic viscous case, the reference values were obtained using adaptive h-refinements, with number of solution degrees of freedom of around 5.1×10^5 and 2.0×10^5 for drag coefficient,

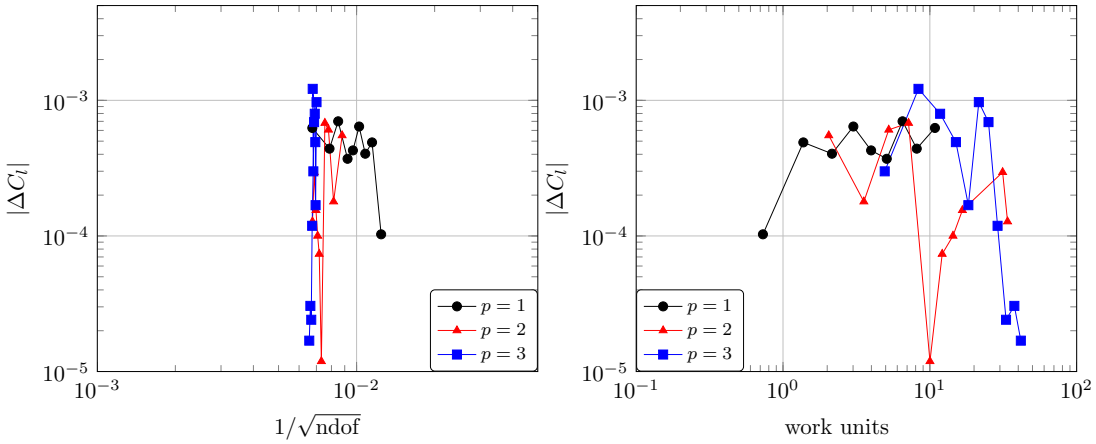

(a) Error in lift coefficient Vs Degrees of freedom

(b) Error in lift coefficient Vs Work units

Figure 4: Inviscid subsonic flow, $M_\infty = 0.5$, $\alpha = 2^\circ$

$c_{d_{ref}}$ and lift coefficient, $c_{l_{ref}}$, respectively. They are given as

$$c_{d_{ref}} = 5.531683 \times 10^{-2} \tag{6}$$

$$c_{l_{ref}} = 1.827345 \times 10^{-1} \tag{7}$$

Fig. 8 shows the drag-adapted mesh after 7 adaptations for $p = 2$. Fig. 9 shows the convergence of the error in the drag coefficient as we vary the polynomial degree. Like in the subsonic inviscid case, higher p increases the convergence rate till $p = 3$. In terms of the work units too, higher p (till $p = 3$) seems to pay off. Fig. 10 shows the convergence of the error in the lift coefficient for different polynomial degrees. Beyond $p = 1$, there is hardly any difference in the convergence rate.

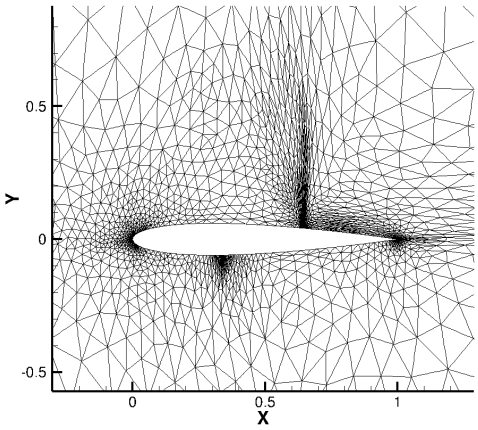

Figure 5: Adapted mesh (4601 elements) for drag coefficient as target function for the inviscid transonic flow

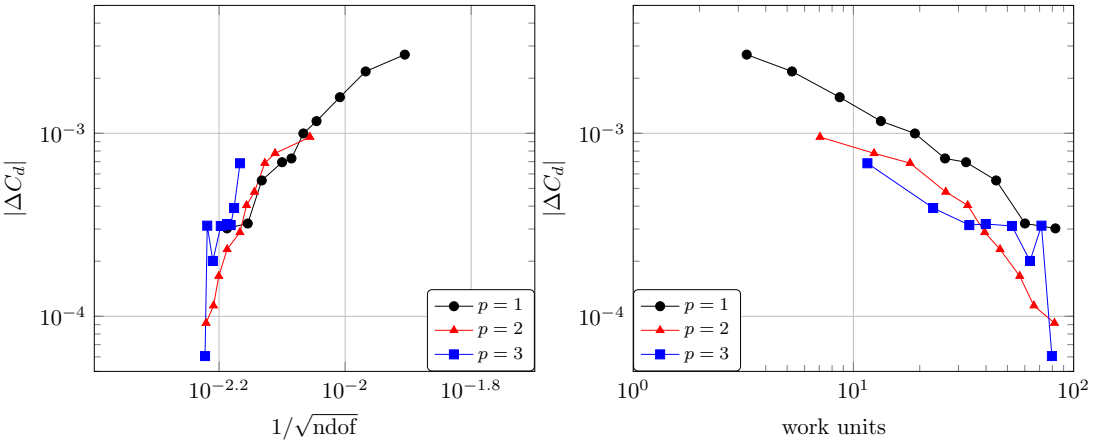

(a) Error in drag coefficient Vs Degree of freedom

(b) Error in drag coefficient Vs Work units

Figure 6: Inviscid transonic flow, $M_\infty = 0.8$, $\alpha = 1.25°$

References

[1] J. Schöberl. Netgen - an advancing front 2d/3d-mesh generator based on abstract rules. *Computing and Visualization in Science*, 1:41–52, 1997.

[2] J. Schütz and G. May. A Hybrid Mixed Method for the Compressible Navier-Stokes Equations. *Journal of Computational Physics*, 240:58–75, 2013.

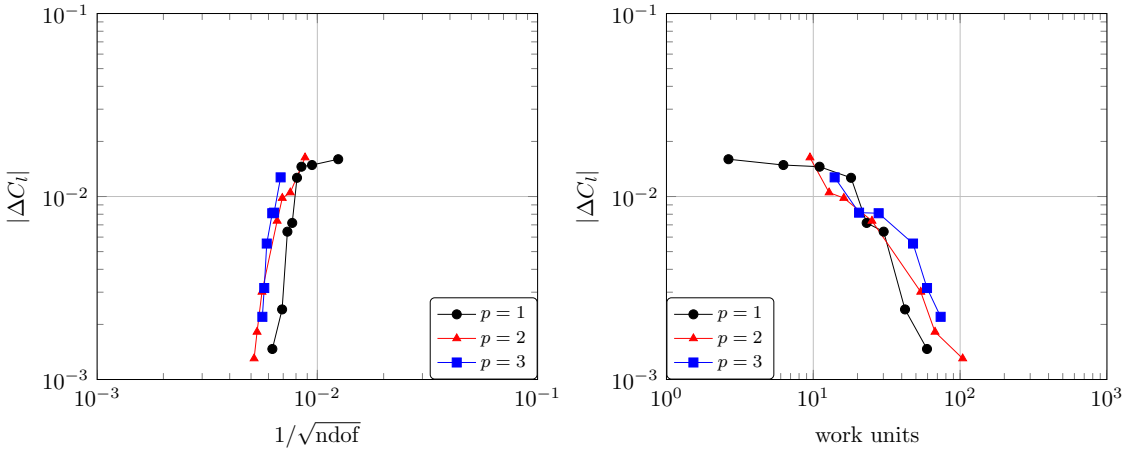

(a) Error in lift coefficient Vs Degrees of freedom

(b) Error in lift coefficient Vs Work units

Figure 7: Inviscid transonic flow, $M_\infty = 0.8$, $\alpha = 1.25°$

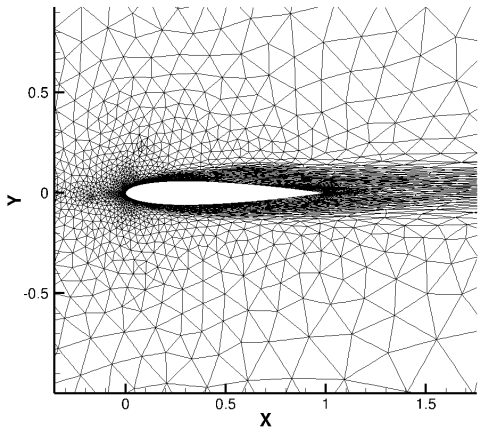

Figure 8: Adapted mesh (8150 elements) for drag coefficient as target function for the laminar flow

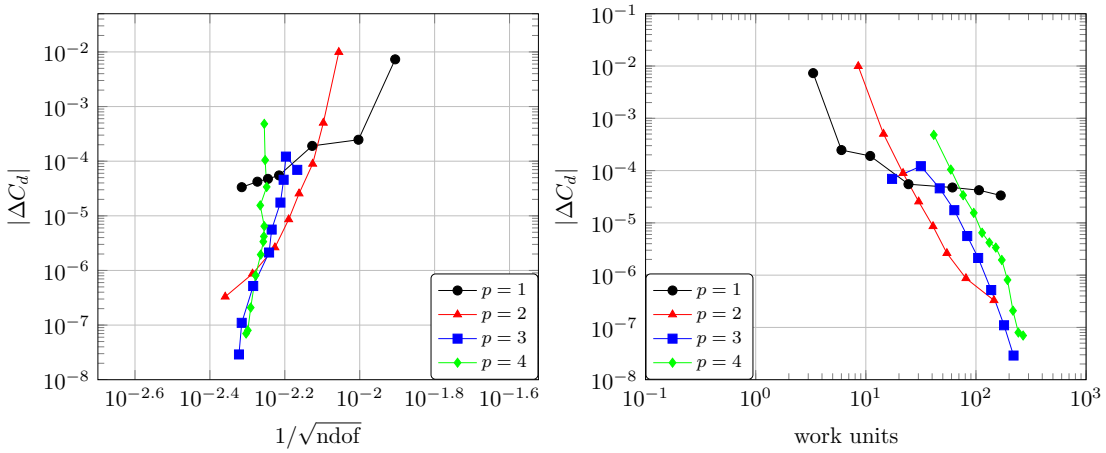

(a) Error in drag coefficient Vs Degrees of freedom

(b) Error in drag coefficient Vs Work units

Figure 9: Viscous laminar flow, $M_\infty = 0.5$, $\alpha = 1°$, Re= 5000

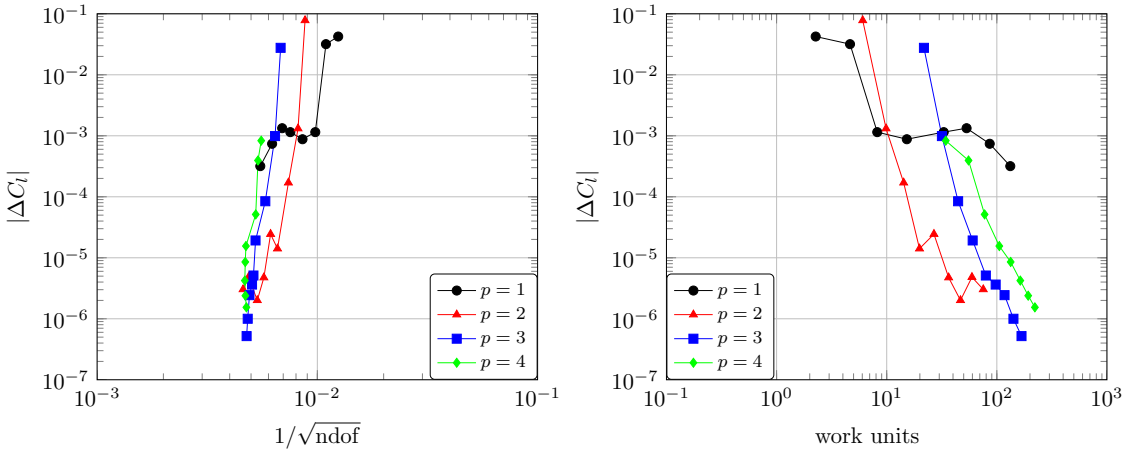

(a) Error in lift coefficient Vs Degrees of freedom

(b) Error in lift coefficient Vs Work units

Figure 10: Viscous laminar flow, $M_\infty = 0.5$, $\alpha = 1°$, Re= 5000